Unveiling Brain Tumors: An Approach Using Graph Theory in Medical Imaging

Nihaas Reddy Ravula, Dheeraj Reddy Balasani, Aishwarya Sudhir, Kartheek Reddy T, Asha Ashok
Department of Computer Science and Engineering, Amrita School of Computing,
Amrita Vishwa Vidyapeetham, Amritapuri, Kerala India
ravulanihaasreddy@gmail.com, dheerajreddy10869@gmail.com, aiswaryasudhir24@gmail.com,
kartheekvishal26@gmail.com, ashaashok@am.amrita.edu

***Abstract*—This research provides a novel method for classifying brain tumours in MRI images that combines graph neural networks (GNN) with convolutional neural networks (CNN). Pre-processed MRI images are translated into graphical representations to capture spatial dependencies, and feature extraction is facilitated by transfer learning with pre-trained CNN architectures. The core model employs a light-weighted network (GAT) to reveal information in network connections, resulting in a valuable learning experience for tumour classification. GAT employs a tracking strategy to choose input from neighbouring individuals, hence enhancing the model's capacity to detect correlations in visual patterns. To better comprehend data features and representations, use qualitative data analysis and visualisation tools. Three versions of this model were created and tested, each based on a different previous CNN design. Overall, our hybrid method shows good potential for brain tumor classification in MRI scans.**

I. Introduction

The importance of early discovery in brain tumour instances cannot be emphasised, since it is critical to successful treatment and a better patient prognosis. This necessity has accelerated the development of computer-assisted detection systems, which provide healthcare workers with sophisticated diagnostic capabilities. One such innovation is the use of graph theory, a powerful approach for analysing the intricate interconnections and patterns found in medical pictures, particularly MRI and CT scans of the brain.

Brain tumours appear as anomalies in the brain's complex network of connections. Despite their importance, conventional image processing approaches may overlook subtle alterations that indicate the existence of small tumours. Graph-based techniques solve this problem by capturing both local changes and the larger context surrounding possible tumours, resulting in more reliable identification.

Using graph theory principles such as nodes, edges, degree distribution, and clusters, we may completely describe tumour connectivity and morphology, including shape, size, and borders. Any deviation from the usual in these qualities can serve as critical warning indications, allowing for early intervention and improved patient outcomes.

The motivation for this research extends beyond the immediate clinical benefits. Brain tumours, whether malignant or benign, place tremendous pressure on the skull, resulting in severe symptoms such as headaches and dizziness. Therefore, early identification is critical to prevent these problems and improve the patient's quality of life.

Furthermore, the successful use of graph-based analysis in detecting brain tumours has far-reaching consequences. It has the potential to accelerate advances in disease modelling and computer-aided diagnostics for a wide range of medical disorders. This research not only intends to expand our understanding of medical image processing using graph theory, but also to encourage expertise in deep learning and graph algorithms, which are becoming increasingly essential in the sectors of healthcare and medical technology.

II. Related Work

Many studies have investigated the use of deep learning techniques in brain tumor classification using MRI images. For example, Mawson et al. Tumors were classified into four groups using a deep neural network (DNN) classifier (PCA). Similarly, Abd-Ellah et al. A two-stage model using a mesh-based network (CNN) for extraction and classification and a region-based CNN for local tumors is proposed. Lakshmi and Hemalatha introduced a computer-aided system (CAD) using PCA and DWT for feature extraction and support vector machine (SVM) for classification. To achieve feature extraction as reported by Casamitjana et al. and a separate group for cancer as described by Saltz et al and Arakeri and Reddy. Pereira et al. While using a fully convolutional 3D approach, Swati et al. Feature extraction using CNN's transformation learning. Additionally, Abiwinanda et al. A hybrid method combining fuzzy and CNN for tumor classification. Sachdeva et al. An advanced neural network method was introduced for accurate tumor classification after removing PCA components. Deepak and Ameer developed various brain tumor models using contour models and ANN techniques. Saw et al. Accuracy was achieved by focusing on the use of GoogleNet for specific inference to classify brain tumors into gliomas, meningiomas, and pituitary tumors. Together, these studies demonstrate the diversity and progression in the distribution of brain tumors.

Diaz-Penas et al. A deep learning method using multiple CNNs has been proposed for brain tumor (CT) classification and segmentation, achieving good results in both tasks. Similarly, Raja proposed an IT classification method that uses hybrid deep autoencoder and Bayesian fuzzy set-based segmentation, resulting in good classification results. Polat

and Güngen investigated a deep transformation method to classify CT from MR images and demonstrated the potential of transformational learning in clinical image analysis. An improved local binary pattern (LBP) feature extraction method for brain tumor classification is investigated, leading to accuracy. Kang et al. A combined method with deep features and machine learning is proposed for MRI-based brain tumor classification, outperforming individual methods. Alzubaidi et al. Meet MedNet, a promising pre-CNN model for CT classification, specifically for medical activities. Riza et al. A deep learning-based IT classification method is proposed using a set of models to improve performance.

Lakshmi and Nagaraja Rao developed a deep learning method for CT MRI classification and achieved good results. Ge et al. Using Coupled GANs to reveal information about the distribution of cancer cells in the brain molecule, thus improving the overall model. Arif et al. A CT detection and classification system was developed using bioinspired orthogonal wavelet transform and deep learning. While Budati and Katta introduce IT detection and classification with IoT, Dehkordi et al. An evolutionary CNN is proposed for improved IT detection and classification. An improved regional development for CT MR image segmentation is proposed, which could help improve classification. Ghasem et al. achieved accuracy improvement by combining deep neural networks with generative adversarial network pre-training for MR image-based CT classification. Recent research in this area has focused on using neural networks to automate feature extraction and normalize the network and transfer learning. However, these methods cannot capture the relationship between pixels; This underscores the need for new methods to incorporate relation-aware representation into CT classification. The motivation and aim of this research is to develop a strategy to interpret the relationship between pixels and create a relationship-aware representation for classification of tumor brain. Relationship-aware representation uses relationships between data points as the knowledge base for effective learning models.

III. Materials and Methods

A. Dataset

MRI data were obtained from Kaggle, which contains approximately 3264 MR images. The MRI , T1, T2 and FLAIR type 35 presented in this document are a combination of different patients and are generally divided into 4 groups: glioma tumor, meningioma tumor, no tumor, pituitary tumor shown in Figure[1]. MRI stands for magnetic resonance imaging. MRI uses magnetic fields instead of X-rays to create detailed images of the body being imaged. Sometimes an MRI can be used to evaluate the size of the tumor. MRI produces better, more detailed images than CT scans and is therefore preferred over CT scans when examining the brain. For the diagnosis of a brain tumor (which may be of primary or secondary origin), MRI of the brain and/or spinal cord may be performed, depending on the type of tumor. This database contains 3094 brain MRIs that distinguish between tumor and non-tumor images.

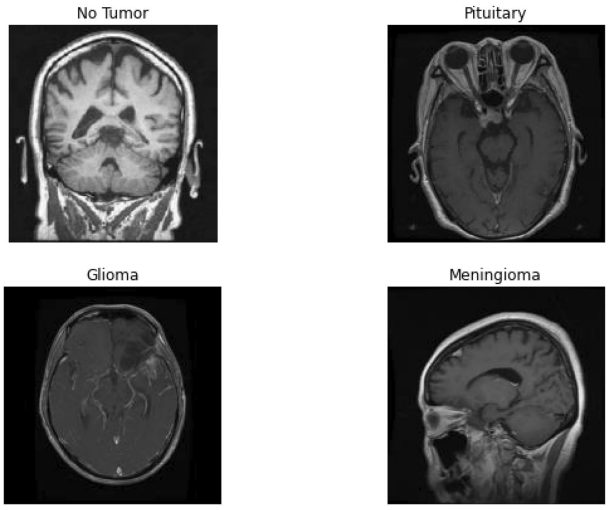

Fig. 1. Brain tumor classes in the dataset

B. Method

Our brain tumor classification system combines Graph neural networks (GNN) and convolutional neural networks (CNN) to effectively model spatial information in MRI images. By treating MRI images as images, we overcome the limitations of regular pixel grid representation, allowing us to capture spatial dependencies and contextual relationships between pixels or areas.

We first processed the MRI images to ensure consistency and quality before training the model. This includes image resolution normalization, intensity normalization, and artifact removal. We also apply image augmentation techniques such as rotation, translation and scaling to enhance data and enhance detail models.

We transform the preprocessed MRI images into graph representations to capture spatial dependencies and contextual relationships. This involves treating image features as nodes and dynamically constructing edges based on a k-nearest neighbor algorithm, thereby establishing connections between regions with similar characteristics.

To accelerate training and enhance feature learning, we employ transfer learning with pre-trained CNN architectures – VGG-16, DenseNet-121, and ResNet-18. These architectures have been trained on large image datasets, enabling us to extract powerful features.

The core of our model consists of the Graph Attention Network (GAT), which uses attention mechanisms to focus on relevant nodes during information dissemination. This allows our model to be more efficient at finding and learning distinctive features that are important for identifying tumors and their boundaries in MRI scans.

We perform data analysis to understand the distribution of tumors throughout the process and identify potential biases. Use visualization techniques such as t-SNE and PCA to explore high-dimensional space and gain insight into representation and class separation.

To identify the optimal backbone architecture for our task, we develop three variations of our core model:

GraphCNN-VGG16: Employs a pre-trained VGG-16 network for feature extraction.

GraphCNN-Densenet121: Leverages a pre-trained DenseNet-121 network, known for its efficient feature reuse and strong performance in image classification.

GraphCNN-Resnet18: Integrates a pre-trained ResNet-18 network, aiming to benefit from residual connections and depth in feature representation.

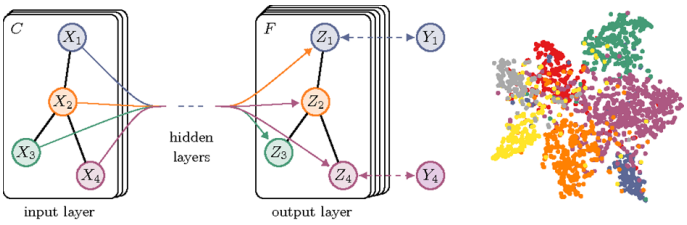

(a) Graph Convolutional Network (b) Hidden layer activations

IV. Implementation

A. Data preprocessing and analysis

The data preprocessing pipeline begins with standardizing the MRI images to ensure consistency and quality. This involves resizing the images to a uniform resolution, applying intensity normalization, and removing any artifacts that may affect the accuracy of the classification task. Additionally, image augmentation techniques such as random cropping, horizontal flipping, and scaling are applied to augment the dataset, thereby enhancing the model's generalization capabilities.

Thorough data analysis is conducted to gain insights into the characteristics of the dataset. Visualization techniques such as bar graphs are utilized to depict the distribution of tumor categories in both the training and testing datasets shown in Figure[2]. This analysis provides valuable information about the balance of classes and potential biases that may exist within the dataset. Moreover, visualization of random samples from the dataset enables visual inspection of the MRI images and their corresponding labels, aiding in understanding the data's structure and identifying any potential anomalies.

V. Model Architecture

Our models share a common structure:

- Feature Extraction: One of VGG-16, DenseNet-121, or ResNet-18 extracts initial image features.
  - VGG-16:The network architecture operates on 224 x 224 RGB images, initially subjecting them to a pre-processing step involving mean subtraction for RGB value normalization. It comprises multiple stacks of convolutional layers, each stack featuring several convolutional layers with 3 x 3 receptive fields. These stacks vary in the number of filters per layer, with the first two stacks housing 64 filters,

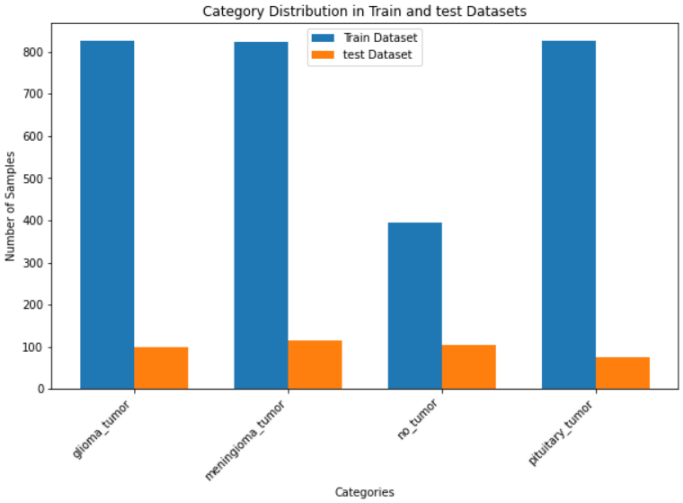

Fig. 2. Distribution in Training and Testing Datasets

the third consisting of three layers with 256 filters, and the final two stacks containing three layers each with 512 filters. Convolutional layers maintain spatial resolution with a fixed stride of 1 pixel and padding of 1 pixel, followed by Rectified Linear Unit (ReLU) activation functions to introduce non-linearity. The GAT layers capture the contextual relationships between nodes in the graph, allowing for adaptive feature learning based on attention mechanisms. This enables the model to focus on relevant regions while processing the image features extracted by the convolutional layers.

To downsample feature maps and reduce computational complexity, max-pooling is employed after every two convolutional layers, utilizing 2 x 2-pixel regions with a stride of 2 pixels. This pooling operation effectively halves the size of the feature maps at each stage. Consequently, after traversing all stacks, the final output size is 7 x 7 x 512, representing both the spatial dimensions and the number of filters in the resulting feature maps.

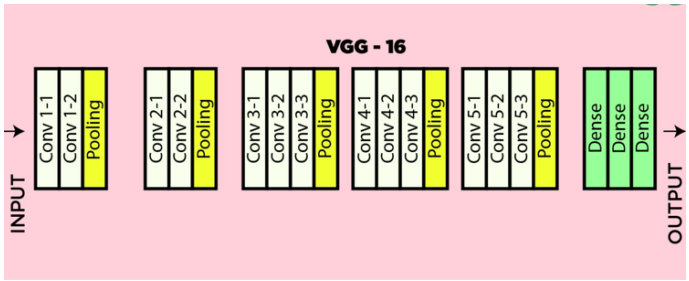

Fig. 3. VGG-16

  - DenseNet-121 Graph Attention Network (GAT) and Convolutional Neural Network (CNN) architecture, namely Dense Convolutional Network, are combined

in the GDenseNet121-GAT model. The goal of this integration is to maximise feature interaction by directly linking all layers and optimising information flow across them. DenseNet121's dense connections are used to condense features through concatenation before passing them to next layers. In contrast to conventional CNNs, these links allow for strong feature propagation and improve feature reuse across the network, which results in effective parameter utilisation.

Through the integration of DenseNet121 into the GAT framework, the model effectively disseminates information across graph nodes through attention mechanisms, facilitating the extraction of complex spatial characteristics from images of brain tumours.By enabling the model to concentrate on pertinent graph regions, the attention mechanism improves the model's capacity to identify minute patterns and variances in tumour features. In the end, this synergistic strategy improves the model's performance in brain tumour classification tasks by facilitating thorough feature extraction and fostering a deeper grasp of the underlying tumour features.

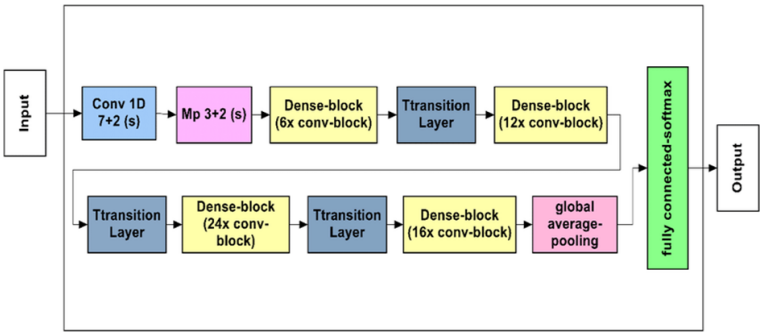

Fig. 4. DenseNet-121

– ResNet-18 An inventive combination of the ResNet-18 architecture and the Graph Attention Network (GAT) framework is exemplified by the GResNet18-GAT model. The model attempts to take advantage of ResNet18's residual connections (Figure [8]), which are well-known for their ability to mitigate the vanishing gradient problem, by incorporating it into the GAT structure. In order to train deeper networks and enable more efficient learning of complicated characteristics, residual connections provide alternate pathways for gradient movement. The unique architecture of ResNet-18 is made up of several residual building blocks with identity mappings and convolutional layers in each. These building pieces facilitate effective feature extraction and hierarchical representation learning by promoting smooth information flow throughout the network. Furthermore, ResNet-18 has become well-known in both academia and business for its outstanding results in a variety of computer vision applications, such as semantic segmentation, object detection, and image classification. The GResNet18-GAT model gains these benefits by incorporating ResNet-18 into the GAT framework, improving its performance for tasks related to brain tumour classification and other areas.

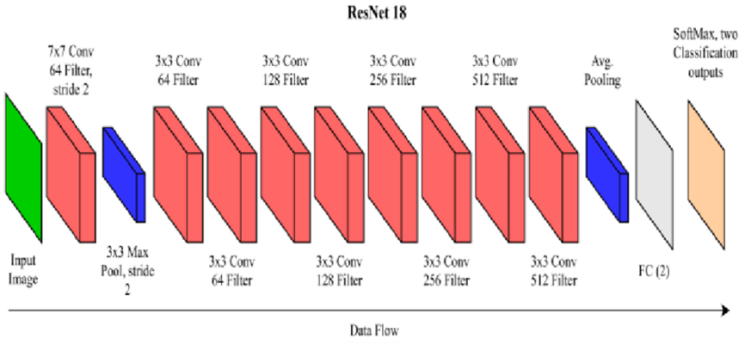

Fig. 5. ResNet-18

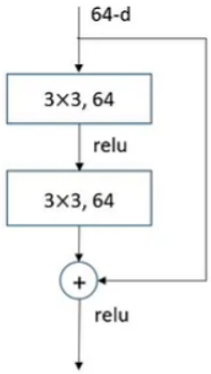

Fig. 6. Residual blocks

- Graph Construction (`convert_graph`):
  - Calculate pairwise distances between extracted feature vectors.
  - Construct a k-nearest neighbor graph to define relationships between image regions.
- GAT Layers (`forward_gcn`): Two GAT layers process the graph, leveraging attention mechanisms to learn spatial features.
- Dropout: Dropout is applied for regularization.
- Output: Models produce classification probabilities for brain tumor classes.

A. *Key Parameters*

- k (graph construction): Number of neighbors per node in the graph used for constructing the k-nearest neighbor graph to define relationships between image regions.
- GAT Layer Dimensionality: Dimension of feature representations in the GAT layers. This parameter determines

the size of the output feature vectors produced by the GAT layers.
- Dropout Rate: Probability within dropout regularization.
- Learning Rate: The rate at which the optimizer adjusts the model parameters during training. It controls the step size in the parameter space search, influencing the convergence and optimization performance of the model.

B. Key Innovations

- Enhanced Image Representation: Our approach overcomes the limitations of traditional pixel grid representations in MRI analysis for tumor classification. By transforming MRI images into graphs, we capture spatial dependencies and contextual relationships, allowing for more effective feature learning.
- Integration of GNN and CNN Strengths: We strategically combine the strengths of Graph Neural Networks (GNNs) and Convolutional Neural Networks (CNNs) in our model architecture. GNNs enable spatial learning by propagating information across graph nodes, while pre-trained CNNs facilitate robust feature extraction from MRI images, leveraging their learned representations from large-scale image datasets.
- Systematic Backbone Exploration: We systematically explore the effectiveness of different backbone architectures, including VGG-16, DenseNet121, and ResNet-18, within our GNN-based brain tumor classification framework. By evaluating the performance of each backbone architecture, we identify the most effective feature extractor for our specific task, optimizing the overall classification accuracy and robustness of the model.

VI. Results and Discussions

In this section, we present the results obtained from the model. The networks were trained successfully and were evaluated using different evaluation metrics.

Lets compare the results between the three models.

VII. Evaluation Metrics

A. Confusion Matrix

It offers a thorough analysis of how the model's predictions and the actual labels for each class compare. There are four sections in the matrix:

- True Positives (TP): Instances where the algorithm correctly predicted a positive output.
- False Positives (FP): Instances where the algorithm predicted a positive output, but the actual output was negative.
- False Negatives (FN): Instances where the algorithm predicted a negative output, but the actual output was positive.
- True Negatives (TN): Instances where the algorithm correctly predicted a negative output.

The model's performance in terms of both accurate and inaccurate predictions can be clearly seen thanks to the confusion matrix, which also offers insights into the model's shortcomings. The ResNet, DenseNet, and VGG-16 matrices are shown below. Figures[7],[8], and [9] display the heatmaps in the same sequence.

$$\begin{bmatrix} 28 & 52 & 20 & 0 \\ 0 & 115 & 0 & 0 \\ 0 & 1 & 104 & 0 \\ 0 & 15 & 6 & 53 \end{bmatrix}$$

$$\begin{bmatrix} 28 & 53 & 19 & 0 \\ 0 & 115 & 0 & 0 \\ 0 & 1 & 104 & 0 \\ 0 & 14 & 6 & 54 \end{bmatrix}$$

$$\begin{bmatrix} 28 & 50 & 22 & 0 \\ 0 & 115 & 0 & 0 \\ 0 & 2 & 103 & 0 \\ 0 & 14 & 6 & 54 \end{bmatrix}$$

B. ROC curves

The ROC (Receiver Operating Characteristic) curve is a graphical representation of a binary classification model's diagnostic capacity under various threshold levels. It compares the true positive rate (TPR) to the false positive rate (FPR) at different thresholds. A ROC curve plots True Positive Rate (TPR), often called sensitivity or recall, on the y-axis. It indicates the fraction of actual positive cases that the model accurately identified as positive. The x-axis depicts the False Positive Rate (FPR). It indicates the percentage of true negative cases that the model mistakenly identified as positive. They are depicted in Figures [13], [15], and [14], respectively.

C. Loss and Accuracy

Accuracy is one of the most commonly used metrics for assessing categorization methods. It assesses the model's ability to properly forecast an observation's class among all observations. In classification tasks, loss is commonly defined as the difference between predicted class probabilities and true class labels. Lower loss numbers indicate higher performance, implying that the model's predictions are more accurate. They are depicted in Figures [10], [11], and [12].

TABLE I
Test Accuracy for Different Models

Model	Test Accuracy
GraphCNN_VGG16	0.796954
GraphCNN_Densenet121	0.667513
GraphCNN_Resnet18	0.756345

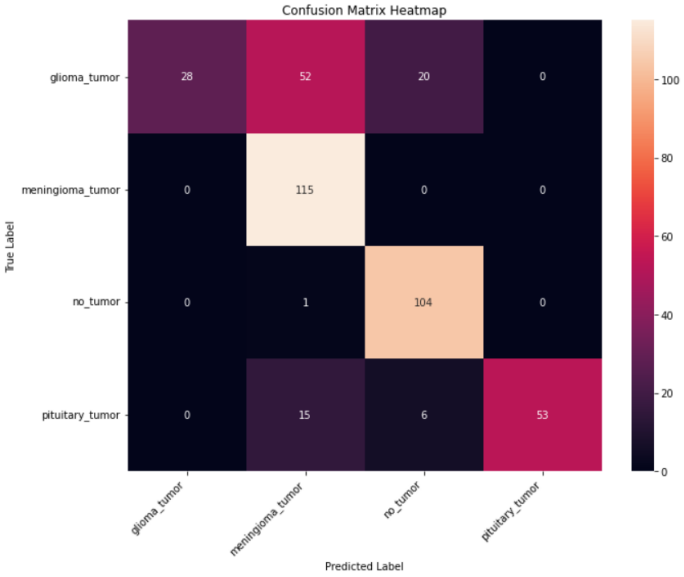

Fig. 7. Confusion Matrix HeatMap for ResNet

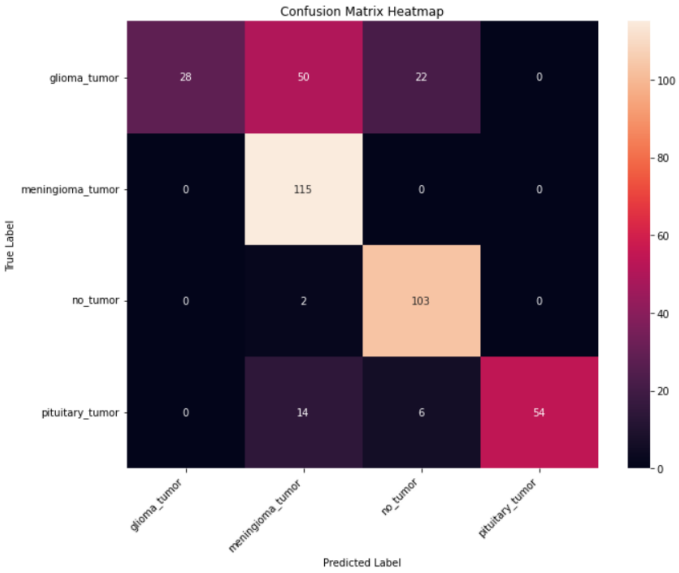

Fig. 9. Confusion Matrix HeatMap for VGG-16

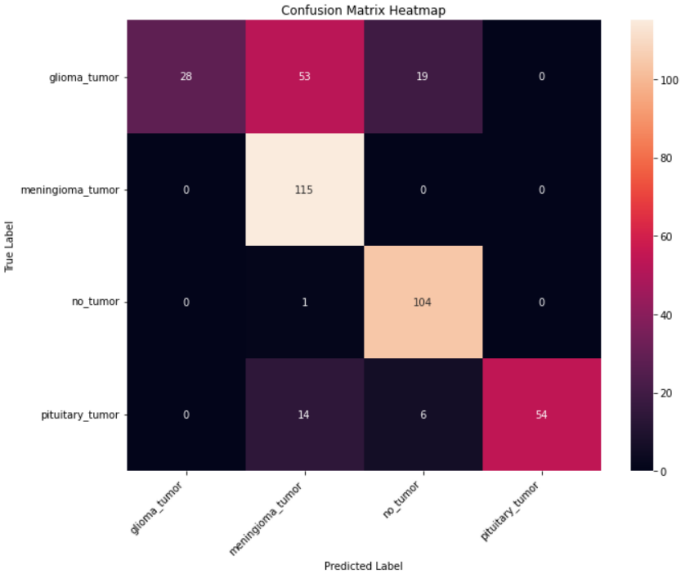

Fig. 8. Confusion Matrix HeatMap for DenseNet

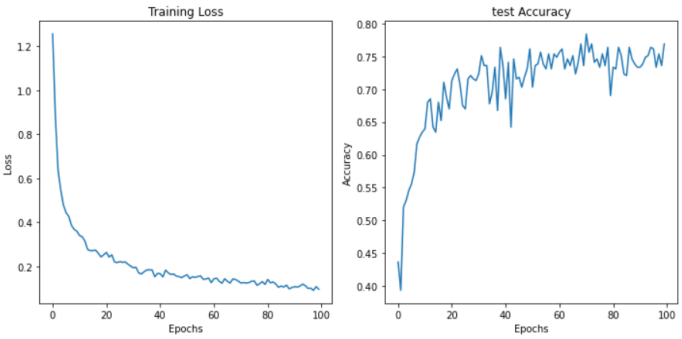

Fig. 10. Loss and Accuracy curves for ResNet

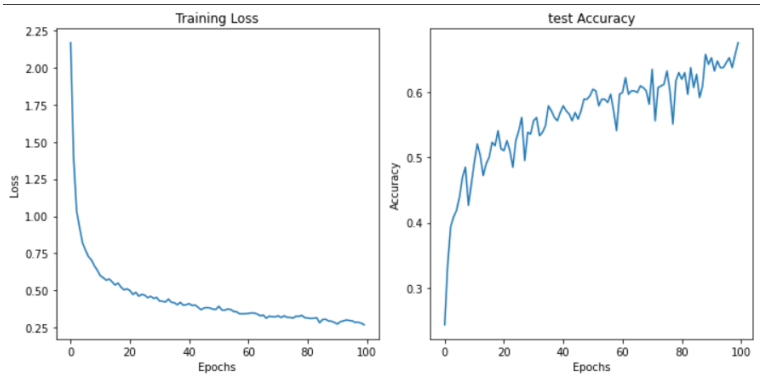

Fig. 11. Loss and Accuracy curves for Densenet

Classification Report

The following are the Classification Reports of ResNet, DenseNet, VGG-16 respectively.

	Precision	Recall	F1-score	Support
Class 0	1.00	0.28	0.44	100
Class 1	0.63	1.00	0.77	115
Class 2	0.80	0.99	0.89	105
Class 3	1.00	0.72	0.83	74
Accuracy			0.76	394
Macro Avg	0.86	0.75	0.73	394
Weighted Avg	0.84	0.76	0.73	394

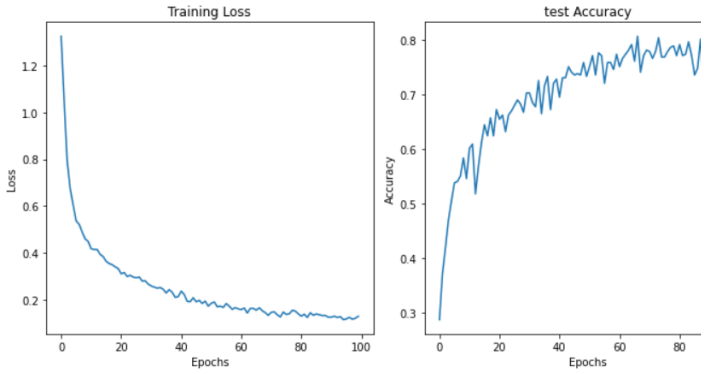

Fig. 12. Loss and Accuracy curves for VGG-16

	Precision	Recall	F1-score	Support
Class 0	1.00	0.28	0.44	100
Class 1	0.63	1.00	0.77	115
Class 2	0.81	0.99	0.89	105
Class 3	1.00	0.73	0.84	74
Accuracy			0.76	394
Macro Avg	0.86	0.75	0.74	394
Weighted Avg	0.84	0.76	0.73	394

	Precision	Recall	F1-score	Support
Class 0	1.00	0.28	0.44	100
Class 1	0.64	1.00	0.78	115
Class 2	0.79	0.98	0.87	105
Class 3	1.00	0.73	0.84	74
Accuracy			0.76	394
Macro Avg	0.86	0.75	0.73	394
Weighted Avg	0.84	0.76	0.73	394

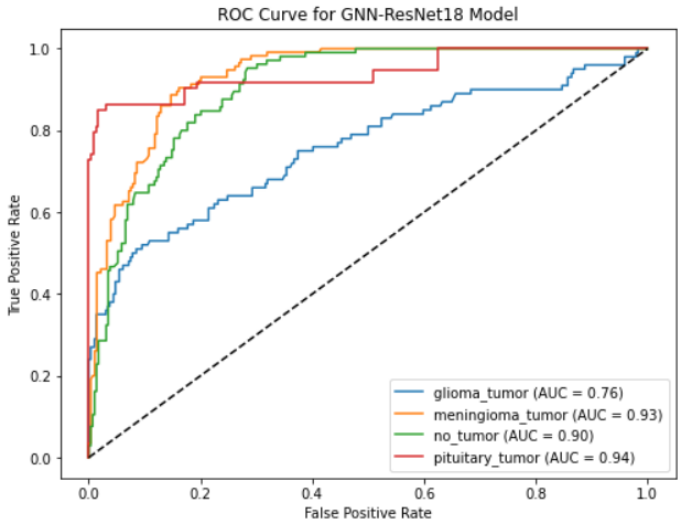

Fig. 13. ROC curves

VIII. Comparison and Findings

In this section, we compare the performance of our Graph Attention Network (GAT) models employing different backbone architectures, notably VGG-16, DenseNet121, and ResNet-18, for brain tumour classification in MRI scans. We compare our findings to those from our earlier studies using Graph Convolutional Networks (GCNs) employing the same architectures, to better understand the influence of switching from GCNs to GATs on classification accuracy.

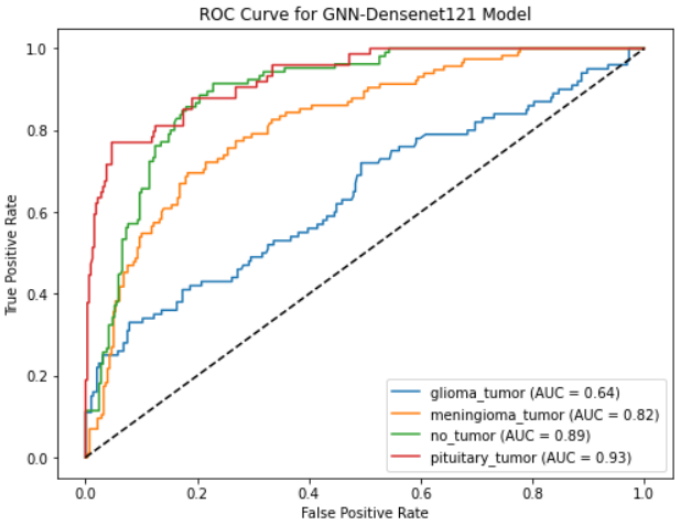

Fig. 14. ROC curves

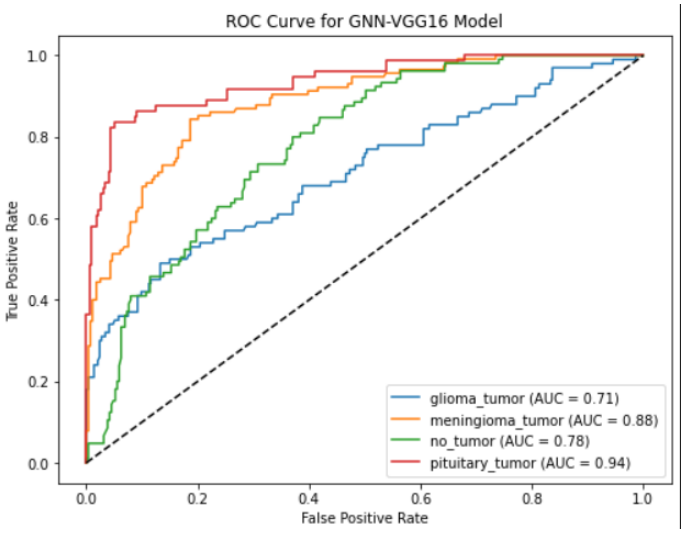

Fig. 15. ROC curves

A. Comparison of GAT Models

GraphCNN_VGG16: With the introduction of GATs, the GraphCNN_VGG16 model exhibits a substantial improvement in test accuracy, achieving a remarkable accuracy of 79.69% from 71.31% . This signifies the efficacy of GATs in capturing complex spatial dependencies within MRI images, leading to enhanced feature representations.

GraphCNN_Densenet121: The GraphCNN_Densenet121 model improves the accuracy from 64.21% to 66.75%. This suggests that the dense connectivity pattern inherent in

DenseNet121 architecture synergizes well with the spatial learning capabilities of GATs.

GraphCNN_Resnet18: Similarly, the GraphCNN_Resnet18 model exhibits a notable increase in test accuracy with the adoption of GATs, achieving an accuracy of 75.63% from 71.57%.

TABLE II
TEST ACCURACY FOR GAT MODEL

Model	Test Accuracy
GAT_VGG16	0.796954
GAT_Densenet121	0.667513
GAT_Resnet18	0.756345

TABLE III
TEST ACCURACY OF GCN MODEL

Model	Test Accuracy
GraphCNN_VGG16	0.713198
GraphCNN_Densenet121	0.642132
GraphCNN_Resnet18	0.715736

B. Comparative Analysis

When GAT models are compared to their GCN counterparts, a consistent trend of improved accuracy emerges across all backbone designs. The inclusion of attention mechanisms in GATs improves information propagation and feature learning, resulting in better classification performance.

IX. CONCLUSION

Our findings demonstrate the effectiveness of GATs in harnessing spatial dependencies in MRI images to accurately classify brain tumours. The synergy between GNNs and CNNs, especially when combined with attention processes, improves the model's ability to detect subtle patterns and fluctuations in tumour features.

The choice of backbone architecture is critical in deciding the model's performance, with VGG-16 emerging as the best performer in our tests. However, DenseNet121 and ResNet-18 both perform well, demonstrating GATs' adaptability in supporting various network architectures.

REFERENCES

1) Deepak, S. & Ameer, P. M. Brain tumor classification using deep CNN features via transfer learning. *Comput. Biol. Med.* 111, 103345 (2019).
2) Sajjad, M. et al. Multi-grade brain tumor classification using deep CNN with extensive data augmentation. *J. Comput. Sci.* 30, 174182 (2019).
3) Mehrotra, R., Ansari, M. A., Agrawal, R. & Anand, R. S. A transfer learning approach for AI-based classification of brain tumors. *Mach. Learn. Appl.* 2, 100003 (2020).
4) Ullah, Z., Farooq, M. U., Lee, S. H. & An, D. A hybrid image enhancement based brain MRI images classification technique. *Med. Hypotheses* 143, 109922 (2020).
5) Çinar, A. & Yildirim, M. Detection of tumors on brain MRI images using the hybrid convolutional neural network architecture. *Med. Hypotheses* 139, 109684 (2020).
6) Díaz-Pernas, F. J., Martínez-Zarzuela, M., Antón-Rodríguez, M., & González-Ortega, D. A deep learning approach for brain tumor classification and segmentation using a multiscale convolutional neural network. *Healthcare* 9(2), 153 (MDPI, 2021).
7) Raja, P. S. Brain tumor classification using a hybrid deep autoencoder with Bayesian fuzzy clustering-based segmentation approach. *Biocybern. Biomed. Eng.* 40(1), 440–453 (2020).
8) Polat, Ö. & Güngen, C. Classification of brain tumors from MR images using deep transfer learning. *J. Supercomput.* 77(7), 7236–7252 (2021).
9) Kaplan, K., Kaya, Y., Kuncan, M. & Ertunç, H. M. Brain tumor classification using modified local binary patterns (LBP) feature extraction methods. *Med. Hypotheses* 139, 109696 (2020).
10) Kang, J., Ullah, Z. & Gwak, J. Mri-based brain tumor classification using ensemble of deep features and machine learning classifiers. *Sensors* 21(6), 2222 (2021).
11) Alzubaidi, L. et al. (2021). MedNet: Pre-trained convolutional neural network model for the medical imaging tasks. *arXiv: 2110.06512*.
12) Raza, A. et al. A hybrid deep learning-based approach for brain tumor classification. *Electronics* 11(7), 1146 (2022).
13) Lakshmi, M. J. & Nagaraja Rao, S. Brain tumor magnetic resonance image classification: A deep learning approach. *Soft. Comput.* 26(13), 6245–6253 (2022).
14) Ge, C., Gu, I. Y. H., Jakola, A. S. & Yang, J. Enlarged training dataset by pairwise GANs for molecular-based brain tumor classification. *IEEE Access* 8, 22560–22570 (2020).
15) Arif, M. et al. Brain tumor detection and classification by MRI using biologically inspired orthogonal wavelet transform and deep learning techniques. *J. Healthc. Eng.* 2022, 1–8 (2022).
16) Budati, A. K. & Katta, R. B. An automated brain tumor detection and classification from MRI images using machine learning techniques with IoT. *Environ. Dev. Sustain.* 24(9), 10570–10584 (2022).
17) Dehkordi, A. A., Hashemi, M., Neshat, M., Mirjalili, S. & Sadiq, A. S. (2022). Brain tumor detection and classification using a new evolutionary convolutional neural network. *arXiv: 2204.12297*.
18) Biratu, E. S. et al. Enhanced region growing for brain tumor MR image segmentation. *J. Imaging* 7(2), 22 (2021).
19) Ghassemi, N., Shoeibi, A. & Rouhani, M. Deep neural network with generative adversarial networks pre-training for brain tumor classification based on MR images. *Biomed. Signal Process. Control* 57, 101678 (2020).